INFECTION AND IMMUNITY, May 2008, p. 2202–2211 Vol. 76, No. 5
0019-9567/08/$08.00+0 doi:10.1128/IAI.01704-07

Vibrio parahaemolyticus Inhibition of Rho Family GTPase Activation Requires a Functional Chromosome I Type III Secretion System▽

Timothy Casselli,† Tarah Lynch,† Carolyn M. Southward, Bryan W. Jones, and Rebekah DeVinney*

Department of Microbiology and Infectious Diseases, University of Calgary, Calgary, Alberta, Canada

Received 20 December 2007/Returned for modification 11 January 2008/Accepted 4 March 2008

***Vibrio parahaemolyticus* is a leading cause of seafood-borne gastroenteritis; however, its virulence mechanisms are not well understood. The identification of type III secreted proteins has provided candidate virulence factors whose functions are still being elucidated. Genotypic strain variability contributes a level of complexity to understanding the role of different virulence factors. The ability of *V. parahaemolyticus* to inhibit Rho family GTPases and cause cytoskeletal disruption was examined with HeLa cells. After HeLa cells were infected, intracellular Rho activation was inhibited in response to external stimuli. In vitro activation of Rho, Rac, and Cdc42 isolated from infected HeLa cell lysates was also inhibited, indicating that the bacteria were specifically targeting GTPase activation. The inhibition of Rho family GTPase activation was retained for clinical and environmental isolates of *V. parahaemolyticus* and was dependent on a functional chromosome I type III secretion system (CI-T3SS). GTPase inhibition was independent of hemolytic toxin genotype and the chromasome II (CII)-T3SS. Rho inhibition was accompanied by a shift in the total actin pool to its monomeric form. These phenotypes were abrogated in a mutant strain lacking the CI-T3S effector Vp1686, suggesting that the inhibiting actin polymerization may be a downstream effect of Vp1686-dependent GTPase inhibition. Although Vp1686 has been previously characterized as a potential virulence factor in macrophages, our findings reveal an effect on cultured HeLa cells. The ability to inhibit Rho family GTPases independently of the CII-T3SS and the hemolytic toxins may provide insight into the mechanisms of virulence used by strains lacking these virulence factors.**

Vibrio parahaemolyticus is a gram-negative halophilic bacterium that is found in estuarine waters worldwide (41). Although this organism has become a leading cause of seafood-borne gastroenteritis due to its accumulation in filter-feeding shellfish (6, 13, 29, 45), its virulence mechanisms remain poorly understood. The hemolytic toxins TDH and TRH are produced by some strains of *V. parahaemolyticus* and have been associated with pathogenesis (41, 59). Genome sequencing of the Asian pandemic strain RMD2210633 has revealed the presence of a type III secretion system on each of the two chromosomes, chromosome I and II (CI-T3SS and CII-T3SS) (38), and several type III secreted proteins have been implicated as potential virulence factors (9, 31, 34, 50, 61). Although studies of secreted proteins have provided further insight into virulence, they have been predominantly restricted to the Asian pandemic strains. There is tremendous genetic diversity among strains of *V. parahaemolyticus*, particularly between Asian strains and those isolated in North America (14, 36). Genotyping of clinical isolates has revealed that the presence of the CII-T3SS and toxin genes is variable among strains, suggesting that these virulence factors are not strictly required to cause disease in humans (39). Because our understanding of the virulence mechanisms of this organism is limited, effectively screening for and identifying these potentially pathogenic isolates is a problem.

* Corresponding author. Mailing address: University of Calgary, 3330 Hospital Dr. NW, Calgary, AB T2N 4N1, Canada. Phone: (403) 220-4095. Fax: (403) 270-2772. E-mail: rdevinne@ucalgary.ca.
† These authors contributed equally to this report.
▽ Published ahead of print on 17 March 2008.

Previous work from our laboratory demonstrated the abilities of North American clinical and environmental isolates of *V. parahaemolyticus* to cause cytoskeletal disruption and the loss of tight junction structures in CaCo-2 cells in a toxin-independent manner (36). Cytoskeletal disruption is a common virulence strategy among pathogenic bacteria and is often mediated by targeting Rho family GTPases (23). Rho family GTPases (Rho, Rac, and Cdc42) act as binary molecular switches, alternating between active GTP-bound and inactive GDP-bound states. This activity allows for the regulation of intracellular signal transduction pathways involved in the transcriptional regulation of cell cycle control, cell trafficking, and cytoskeletal organization (see 28 for a review of Rho family GTPase biochemistry and biology). With regard to the actin cytoskeleton, Rho family GTPases mediate the intracellular formation and organization of actin stress fibers and the cellular protrusions lamellipodia and filopodia. Activation of these signaling molecules can lead to the polymerization of actin monomers (G-actin) to form filamentous actin (F-actin). Rho activation stimulates formin-induced actin nucleation during stress fiber formation (28, 52, 54, 64), whereas the activation of Rac and Cdc42 induces F-actin polymerization during the formation of lamellipodia and filopodia, respectively, through the activation of the Arp2/3 complex (15, 25, 28). Active Rho, Rac, and Cdc42 may also serve to inhibit the ADF/cofilin-dependent depolymerization of F-actin to G-actin through the subsequent activation of LIM kinases (8, 16, 37, 48). The inactivation of Rho family GTPases can lead to depolymerization of actin structures (7, 28) and an overall loss of intracellular F-actin (17, 46, 58) and will inevitably affect cell-cell and cell-matrix adhesion sites (12, 47).

TABLE 1. PCR profiling of virulence factors of strains used in this study

V. parahaemolyticus strain	Presence or absence of virulence factor[a]:			
	TDH	TRH	CI-T3SS	CII-T3SS
BCC23	+	−	+	+
BCC23Δ*vscN1*	+	−	*	+
BCC23Δ*vscN1*-compVp1686	+	−	*	+
BCC23Δ*vscN2*	+	−	+	**
BCC23ΔVp1686	+	−	+	+
BCC23ΔVp1686-comp	+	−	+	+
BCC23Δvp1686-compΔFic	+	−	+	+
BCC7	+	+	+	−
BCC34	−	−	+	−
BCE306	−	−	+	−
BCE515	−	−	+	−

[a] The presence (+) or absence (−) of TDH-related hemolysin (TDH), thermostable direct hemolysin (TRH), and CI- and CII-T3SS strains was determined by PCR. *, isogenic mutant strain Δ*vscN1*, with a deletion introduced in the gene encoding the ATPase portion of the secretion apparatus. **, isogenic mutant strain Δ*vscN2*, with a deletion introduced in the gene encoding the ATPase portion of the secretion apparatus.

The regulated activation of Rho family GTPases involves several accessory molecules. Inactive GDP-bound GTPases reside in the cytoplasm bound to GDP dissociation inhibitors (GDIs). When they are properly stimulated, the GTPases are targeted to the cell membrane where guanine nucleotide exchange factors (GEFs) catalyze the exchange of GDP for GTP, as well as the dissociation from the GDI. This nucleotide exchange causes a conformational change in the GTPase to its active form, allowing interaction with downstream effector molecules. GTPase-activating proteins (GAPs) then catalyze the intrinsic ability of the GTPase to cleave the γ-phosphate of GTP via hydrolysis, thereby returning the protein to its GDP-bound inactive state (28). Bacterial pathogens often mimic or inhibit the steps in this cycle in order to facilitate virulence (3, 5, 56, 62).

In this study, we examined the effect of North American isolates of *V. parahaemolyticus* on Rho family GTPases in cultured HeLa cells. Infection with clinical and environmental isolates resulted in the in vivo inhibition of Rho activation in response to the stimulus calpeptin, as well as inhibition of the in vitro activation of Rho family GTPases isolated from cell lysates. GTPase inhibition was accompanied by a shift in the pool of intracellular actin to its monomeric form. These phenotypes were dependent on the translocation of Vp1686 into the HeLa cells via a functional CI-T3SS, a novel effect of this previously characterized protein. The delivery of this potential virulence factor by nontoxigenic strains supports evidence for their potential to cause disease in humans and illustrates the need for a better understanding of virulence.

MATERIALS AND METHODS

Bacterial strains and cell lines. *Vibrio parahaemolyticus* clinical isolates BCC23, BCC34, and BCC7 and environmental isolates BCE306 and BCE515 were generous gifts from the Canadian Food Inspection Agency (Burnaby, BC, Canada) (Table 1). Cultures were grown at 37°C for 18 h with shaking (225 rpm) in nutrient broth (Difco, Sparks, MD) supplemented with 3% NaCl (SNB). HeLa cells (CCL2; ATCC) were grown in Dulbecco's modified Eagle's medium (DMEM; catalog no. 11965; Invitrogen, Carlsbad, CA) supplemented with 10% fetal bovine serum at 37°C in 5% CO_2, unless otherwise specified.

Rho quantification enzyme-linked immunosorbent assay. Assays were performed using an absorbance-based G-LISA RhoA activation assay kit (Cytoskeleton, Denver, CO) following the manufacturer's instructions. Briefly, HeLa cells were seeded in 6-well plates and allowed to reach 50 to 60% confluence, at which point they were rinsed with phosphate-buffered saline (PBS) and serum starved (DMEM, no supplementation) for 24 h. For infection studies, cells were infected with bacterial overnight cultures (multiplicity of infection [MOI], 25) for the specified times. After appropriate infection times, the monolayers were rinsed again with PBS and treated with DMEM supplemented with either 0.1 mg/ml calpeptin (Biomol, Plymouth Meeting, PA) to stimulate Rho activation or with dimethyl sulfoxide (DMSO) medium control for 20 min. The monolayers were then rinsed with PBS and lysed in 100 μl of lysis buffer, and lysates were immediately snap frozen in liquid nitrogen to prevent spontaneous Rho inactivation. Once all samples had been processed, lysates were thawed, normalized for protein concentration, and added to 96-well plates coated with Rhotekin-RBD to bind activated Rho. Wells were washed in order to remove inactive Rho, incubated with primary and secondary antibodies as per instructions, and treated with a horseradish peroxidase detection reagent. The amount of activated Rho was determined by measuring the optical density at 490 nm (OD_{490}) in a plate reader (Bio-Rad 680 microplate reader). Activated Rho in calpeptin-treated samples was calculated as a ratio of the activated Rho from medium control samples to normalize for variability between assays and expressed as the mean ± standard error of the mean (SEM). A one-way analysis of variance (ANOVA), followed by Dunnett's multiple comparison test, was used to compare infected samples with uninfected controls (GraphPad Prism). A value of $P < 0.05$ indicates significance.

PCR profiling for virulence factors. DNA was isolated, using PCR, from a collection of *V. parahaemolyticus* strains (Table 1) as described previously (36). Primer sequences were used for PCR amplification of the genes *tdh* and *trh* and the genes encoding the ATPase portions of the CI-T3SS (*vscN1*) and CII-T3SS (*vscN2*) as listed in Table 2.

GTPase pulldown assay. Assays were performed using commercially available kits (Upstate, Lake Placid, NY) following the manufacturer's instructions. Briefly, HeLa cells were seeded in 10-cm dishes and allowed to reach 80% to 90% confluence. For infection studies, cells were infected with overnight-incubated bacterial cultures (MOI, 25) for the specified times. The monolayers were rinsed with Tris-buffered saline before 0.5 ml of magnesium lysis buffer (25 mM HEPES [pH 7.5], 125 mM NaCl, 1% Igepal CA-630, 10 mM $MgCl_2$, 1 mM EDTA, and 10% glycerol) supplemented with 1 mM sodium orthovanadate (Sigma-Aldrich, St. Louis, MO) and protease inhibitors (Complete protease inhibitor; Amersham Biosciences United Kingdom Limited, Little Chalfont, Buckinghamshire) was added. Cells were isolated by scraping, and lysates were cleared of insoluble debris by centrifugation (1,136 × *g* for 10 min at 4°C). GTPases were activated by adding an additional 1 mM EDTA and 100 μM GTPγS (Sigma-Aldrich) and incubated at 30°C for 30 min with agitation. Activated Rho was affinity purified using Rhotekin-RBD agarose beads, whereas activated Rac and Cdc42 were isolated by using PAK-1-agarose beads. The beads were washed following the manufacturer's instructions to remove inactive GTPases and other cellular proteins, and the samples were resolved by using sodium dodecyl sulfate (SDS)–12% polyacrylamide gel electrophoresis (PAGE). Proteins were transferred to nitrocellulose and immunoblotted with their specific antisera, using the following modifications to the manufacturer's instructions: Rho samples were probed with the monoclonal antibody provided with the kit (1:500) and washed three times (10 min each wash, Tris-buffered saline). Rac samples were blocked for 1 h at room temperature in 5% skim milk with PBS before they were exposed to the primary antibody (1:1,000) and washed three times (20 min each wash in double-distilled water). Samples for Cdc42 detection were probed with primary antisera (1:500, Becton Dickinson, Franklin Lakes, NJ) and washed three times (2 min each wash with PBS). All samples were then probed with anti-mouse antiserum conjugated to horseradish peroxidase, washed as described above, and visualized by using enhanced chemiluminescence. Samples for measuring the total cellular GTPases were prepared in a similar manner, without the addition of Rhotekin-RBD or PAK-1 agarose.

Mutant construction. (i) Deletion constructs. Primer sets were constructed (Table 2) for overlap extension PCR (26) using Platinum *Pfx* DNA polymerase (Invitrogen) in order to create in-frame deletions in the following genes.

(ii) *vscN1* (Vp1668). A 978-bp fragment upstream of the deleted region was amplified using the primers 1668F_BamHI and WA_R_EcoRI. Similarly, a 984-bp fragment downstream of the deleted region was amplified using the primers 1668R_PstI and WB_F_EcoRI. Amplified products were used as templates in a PCR using 1668F_BamHI and 1668R_PstI to create a 1,962-bp product. Homology of the 5′ to the 3′ ends of WB_R_EcoRI and WA_F_EcoRI facilitated the introduction of an EcoRI restriction site along with a 273-bp

TABLE 2. Oligonucleotides used for PCR screening of virulence factors and mutant construction

Primer	Reference or source	PCR screening of virulence factors (5′→3′)	Mutant construction and complementation (5′→3′)[a]
*tdh*_F	43	CCATCTGTCCCTTTTCCTGCC	
*tdh*_R	43	CCACTACCACTCTCATATGC	
*trh*_F	27	TTGGCTTCGATATTTTCAGTATCT	
*trh*_R	27	CATAACAAACATATGCCCATTTCCG	
*vscN1*_F	35	GGGGCTGTGGTGCCGGGCGTA	
*vscN1*_R	35	GGGGCGATGCCTTTCAGTTGAGC	
*vscN2*_F	35	AAACGTACTCACCGACTCGAATG	
*vscN2*_R	35	TGAAATCGTTAAGGTGACAGGC	
1668F_BamHI			CCC**GGATCC**ACCAGCTCATGCGCTTCGTTAACGCGAACGCCACCG
WA_R_EcoRI			ACGGGTGACGGA**GAATTC**GAAAATGCCCATACGTTGGC
1668R_PstI			CCG**CTGCAG**GGTACTGTTGTTGGCGCGATTGTTCCGCGATTTC
WB_F_EroRI			ATGGGCATTTTC**GAATTC**TCCGTCACCCGTTTTGCTCG
1338F_PstI			A**CTGCAG**CGTCAGAACAATCTCGT
1338R_ApaL1			**GTGCAC**AAGGCAACAACCTTGAAGTGGCTC
ATPout_R_BamH1			**GGATCC**AAGAGTCGTCTACAAAATAAAGTACAAG
ATPout_F_BamH1			**GGATCC**GAATAATCCTAAACGTTGTCCTTCTCCAA
VP1686Del1ApaLI			**GCGGTGCACAGAGAAGCGCTGCAATTGGTG**
VP1686Del2-OE			GCAGTTCAGCGATGGCCTTACCACCAATGCTGAGT
VP1686Del3-OE			GCATTGGTGGTAAGGCCATCGCTGAACTGCGTAAT
VP1686Del4ApaLI			GCG**GTGCAC**CGTCAGTTTATTTTCGCCATT
VP1686PoNPst			GCG**CTGCAG**CCAGTGATGGATGCTAACCAA
VP1686PoCBgl			GCG**AGATCT**TTTGATACCGTGAAGGCTATT
VP1686PoFic_F			TTA **ACG CGT** ATG GGG CGC ATG CTT TAT GCC ATC
VP1686PoFic_R			TTA **ACG CGT** AAA GCC GTG ATA ACC AAT CAC ACC AGC AAA TAA ATG TTT ACC

[a] Restriction endonuclease recognition sites are indicated in boldface type.

deletion within the gene, creating the mutant allele of Vp1668, named Δ*vscN1*. Δ*vscN1* was restriction digested with BamHI and PstI and ligated into the pHSG415-mob construct, which was digested similarly (63).

(iii) *vscN2* (Vpa1338). A deletion within the Vpa1338 gene was created by amplifying a 951-bp fragment upstream of the deleted region, using the primers 1338_F_ PstI and ATPout_R_BamH1, and a 1.4-kb fragment downstream of the deleted region, using the primers 1338_R_ApaL1 and ATPout_F_BamH1 (Table 2). These two fragments were digested with BamHI, ligated together, and PCR amplified (using the 1338_F_PstI and 1338_R_ApaL1 primers) to create a 2.35-kb in-frame fragment containing a 510-bp deletion named Δ*vscN2*. As described above, Δ*vscN2* was digested with PstI and ApaL1 and ligated into the similarly cut pHSG415-mob construct.

(iv) Vp1686. A 1,026-bp PCR product upstream of the deleted region was amplified using the primers VP1686Del1ApaLI and VP1686Del2-OE. The primers VP1686Del4ApaLI and VP1686Del3-OE were used to amplify a 1,056-bp region downstream of the deletion. Amplified products were purified and used as the template to create a 2,082-bp product containing a 991-bp deletion that was ligated into pHSG415-mob using the ApaLI site.

Generation of mutant strains. pHSG415-mob containing each deletion construct was transformed into the mobilizing strain *Escherichia coli* S17-1 (60). Cells were recovered in SOC medium (0.5% yeast extract, 2.0% tryptone, 2.5 mM KCl, 10 mM $MgCl_2$, 20 mM glucose) at 30°C for 2 h and subsequently plated for 36 h at 30°C on Luria broth (LB) agar containing kanamycin (50 μg/ml).

Equal volumes of overnight culture of *V. parahaemolyticus* BCC23 and *E. coli* S17-1 containing one of the constructs pHSG415-mob::Δ*vscN1*, pHSG415-mob::ΔVp1686, or pHSG415-mob::Δ*vscN2* were mixed, centrifuged (4,000 × *g*, 5 min), and resuspended in LB. This mixture was spotted onto SOB agar (0.5% yeast extract, 2.0% tryptone, 2.5 mM KCl, 10 mM $MgCl_2$) supplemented with 1.5% NaCl and incubated at 30°C for 2 h. The mating mixture was resuspended in 50 μl LB and plated on thiosulfate citrate bile sucrose agar containing 125 μg/ml kanamycin. Following a 24-h incubation at 30°C, transconjugants were substreaked onto thiosulfate citrate bile sucrose agar containing kanamycin to ensure no *E. coli* contamination. Mutant strains were selected as described previously (63) and confirmed by PCR screening.

Complementation with Vp1686. Vp1686 was cloned into pONGO, a pACYC184 (New England Biolabs, Ipswich, MA) derivative that has been modified to allow the addition of a C-terminal hemagglutinin (HA) tag and a cassette that enables mobilization (E. Allen-Vercoe and C. M. Southward, unpublished). The primers VP1686PoNPst and VP1686PoCBgl (Table 2) were used to amplify the 1,206-bp DNA fragment encoding Vp1686, whereupon it was restriction digested with PstI and BglII and ligated into similarly digested pONGO to create pONGO::Vp1686. The construct was transformed into *E. coli* S17-1 and conjugated into the deletion strains BCC23ΔVp1686 and BCC23Δ*vscN1* to create BCC23ΔVp1686-comp and BCC23Δ*vscN1*-compVp1686, respectively.

Complementation with Vp1686ΔFic. The primers VP1686PoFic_F and VP1686PoFic_R (Table 2) were used to amplify pONGO::Vp1686, using inverse PCR. The resulting product created a deletion of nucleotides 1,051 to 1,068 in the Vp1686 gene and introduced an AflIII restriction endonuclease recognition sequence at this site. This form of the gene was called Vp1686ΔFic. The resulting product was digested using AflIII and ligated to restore a circular plasmid called pONGO::Vp1686ΔFic. Vp1686ΔFic codes for a protein containing the in-frame deletion of amino acid residues 352 to 355, and the introduction of the AflIII site created a silent mutation in the flanking residues. pONGO::Vp1686ΔFic was transformed into *E. coli* S17-1 and conjugated into the deletion strain BCC23Δ Vp1686 to create BCC23ΔVp1686-compΔFic.

Purification of Vp1686 and antibody production. The coding region of Vp1686 was cloned into the bacterial expression vector pET14b (EMD Biosciences, Inc., Madison, WI), which introduces an amino-terminal six-histidine tag, and trans-

formed into *E. coli* strain BL21(DE3). Bacteria were grown to an OD_{600} of 0.6 prior to the addition of 1 mM isopropyl-β-D-thiogalactopyranoside and grown at 37°C for 1.5 h to induce protein expression. Six-His-Vp1686 was batch purified using nickel agarose (Qiagen, Mississauga, ON, Canada), following the manufacturer's instructions. Purified recombinant protein was used to generate antiserum in rats (24).

Vp1686 translocation assay. HeLa cells were seeded in three 10-cm dishes per sample and allowed to reach 80% to 90% confluence. Cells were infected (MOI, 25) for 2.5 h. The monolayers were recovered using a cell scraper and resuspended in 10 ml of PBS. HeLa cells were washed by centrifugation (195 × *g*, 2 min, 4°C) and resuspended in 10 ml of PBS to remove excess bacteria. After cells were washed three times, pellets were resuspended in 200 μl of PBS supplemented with protease inhibitors (Complete protease inhibitor; Amersham Biosciences). The resuspended cells were passed through a 22.5-gauge needle to mechanically lyse the HeLa cells without causing residual bacterial lysis. This mechanical lysis step was repeated, and the cells were examined under a microscope after each passage until 80 to 90% free nuclei were observed. Samples were cleared of insoluble debris such as unbroken HeLa cells, nuclei, and bacteria by centrifugation (3,000 × *g*, 15 min, 4°C). Proteins from the supernatant were resolved using SDS-12% PAGE, transferred to nitrocellulose, immunoblotted with anti-Vp1686 antisera, and visualized using enhanced chemiluminescence detection.

Bacterial lysates were probed for Vp1686 as a control for protein production. Subcultures were made as 1/12 dilutions of overnight cultures in DMEM with the addition of 20 mM $MgCl_2$ and 20 mM sodium oxalate. The cultures were grown with aeration at room temperature for 2 h and then at 37°C for an additional 3 h to induce the expression of type III secreted proteins (40). Bacteria were pelleted by centrifugation (3,110 × *g*, 15 min, 4°C), resuspended in 5× SDS sample buffer, and resolved using SDS-12% PAGE. Proteins were transferred to nitrocellulose, immunoblotted with anti-Vp1686 antisera, and visualized using enhanced chemiluminescence detection.

G-actin: total actin assay. HeLa cells were seeded in 10-cm dishes and grown to 90% confluence. Cells were infected with overnight bacterial culture (MOI, 25) for 2 h. Monolayers were rinsed with PBS, scraped from the dish, and pelleted by centrifugation (195 × *g*, 5 min, 4°C). Cells were lysed in 200 μl of lysis buffer {1 mM ATP, 50 mM PIPES [piperazine-*N*,*N*′-bis(2-ethanesulfonic acid)], 50 mM NaCl, 5 mM $MgCl_2$, 5 mM EGTA, 5% glycerol, 0.1% Igepal, complete protease inhibitors [Amersham Biosciences]} and incubated at 30°C for 10 min. The samples were ultracentrifuged at 100,000 × *g* for 60 min to separate G-actin and F-actin. Pellets were treated with 200 μl of 1 μM cytochalasin D for 1 h on ice. Both the supernatant and the pellet samples were resolved using SDS-12% PAGE, transferred to nitrocellulose, immunoblotted with anti-actin antisera (Cytoskeleton Inc., Denver, CO), and visualized using enhanced chemiluminescence detection. Actin levels were quantified using densitometry (Rasband, W. S., ImageJ, U.S. National Institutes of Health, Bethesda, MD; http://rsb.info.nih.gov/ij/; 1997 to 2007). G-actin was calculated as the ratio of the total actin signals for each sample and expressed as the means ± standard errors of the means (SEM). A repeated measures one-way ANOVA, followed by Dunnett's multiple comparison test was used to compare infected samples with uninfected controls (GraphPad Prism). A *P* value of <0.05 indicates significance.

RESULTS

***Vibrio parahaemolyticus* inhibits Rho, Rac, and Cdc42 activation.** To determine the effects of *V. parahaemolyticus* infection on Rho family GTPases, intracellular Rho activation was examined in response to stimulation with the Rho activator calpeptin (57). An enzyme-linked immunosorbent assay (ELISA) was used to quantify the amount of activated Rho in HeLa cell monolayers. A sixfold increase in activated Rho was detected in uninfected samples after they were incubated with calpeptin compared to those incubated with control medium alone (Fig. 1A). This increase was not observed when the HeLa cells were infected with clinical and environmental isolates of *V. parahaemolyticus* prior to stimulation with calpeptin (Fig. 1A), indicating that infection was interfering with calpeptin-mediated Rho activation. For most strains, the inhibition of Rho activation occurred after a 2.5-h infection. BCE515 exhibited a delayed time course of Rho inhibition (8-h infection time) due to slower growth (growth data not shown). Rho inhibition was not restricted to calpeptin treatment, as similar results were seen when fetal bovine serum was used to stimulate Rho activation (data not shown).

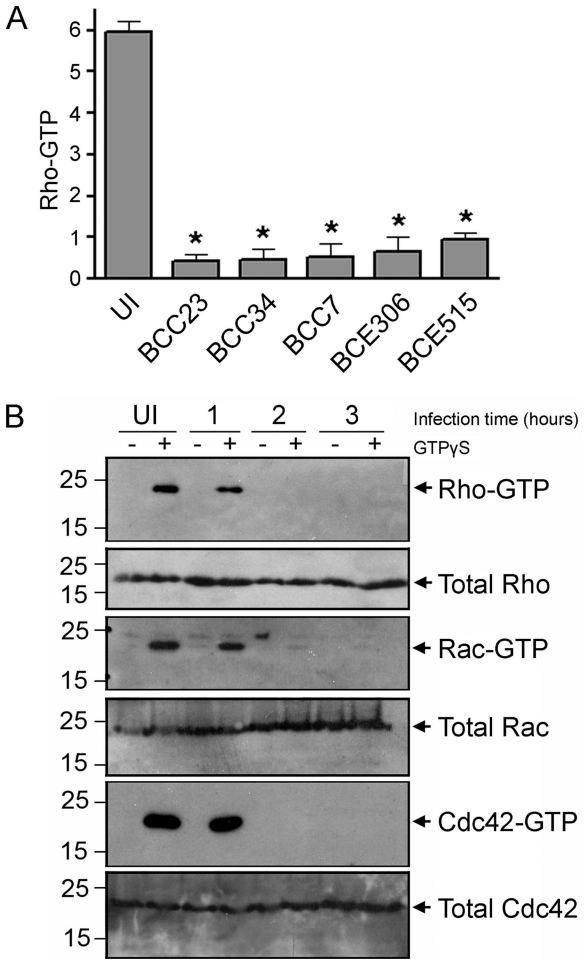

FIG. 1. *V. parahaemolyticus* inhibits Rho family GTPase activation. (A) Activated Rho recovered from lysates of calpeptin-treated HeLa cells, as determined by ELISA. For infection studies, cell monolayers were infected with clinical (BCC23, BCC34, and BCC7) and environmental (BCE306 and BCE515) strains of *V. parahaemolyticus* prior to treatment of the cells with calpeptin. Cells were infected with all strains for 2.5 h before calpeptin treatment, with the exception of E515, which was infected for 8 h. Relative amounts of activated Rho are shown as a ratio of uninfected cells treated with medium control (DMSO) alone ± SEM ($n = 3$). *, $P < 0.001$ by ANOVA. (B) Anti-Rho, Rac, and Cdc42 immunoblots of HeLa cell lysates after cells were infected with *V. parahaemolyticus* BCC23 for the indicated times. Lysates were prepared as described in Materials and Methods and assayed with (+) or without (−) incubation with GTPγS as indicated. Upper panels represent activated GTPase, whereas lower panels represent total cellular GTPase levels. Apparent molecular weights (at left) are in kilodaltons. Data shown are representative of three independent experiments.

Results from the ELISA showed a lack of Rho activation in response to external stimuli after infection with *V. parahaemolyticus*. In order to better understand the nature of this phenotype, a pulldown assay was used to examine the ability to activate Rho family GTPases isolated from HeLa cell lysates after infection with the clinical isolate BCC23. This strain was chosen because it carries the *tdh* gene, as well as genes encod-

ing both the CI- and CII-T3SS (Table 2). Cellular GTPases were irreversibly activated in vitro by incubating HeLa cell lysates with the nonhydrolyzable GTP analogue GTPγS. Activated Rho was detected in uninfected samples; however, it was no longer detected after a 2-h infection with BCC23 (Fig. 1B). Total cellular Rho remained constant over the course of infection (Fig. 1B), indicating that the infection caused interference with Rho activation rather than protein degradation or inhibition of protein expression at the transcriptional or translational level. The inhibition of Rac and Cdc42 activation were also seen after a 2-h infection with BCC23 (Fig. 1B). Due to the limited sensitivity of the assay, levels of activated Rho, Rac, and Cdc42 were not detectable in the absence of GTPγS. The ability to inhibit Rho family GTPase activation through the in vitro incorporation of GTPγS was consistent among the clinical and environmental strains tested in Fig. 1A (data not shown).

GTPase inhibition requires a functional CI-T3SS. *V. parahaemolyticus* virulence has historically been correlated with the production of the hemolytic toxins TDH and TRH (41, 59). Additional potential virulence factors such as the presence of two distinct T3SSs (CI-T3SS and CII-T3SS) have been suggested (38), however their contributions to virulence are not well characterized. PCR screening was used to examine the genetic profiles of clinical and environmental isolates in order to identify the bacterial factors required for GTPase inhibition. Possession of the toxin genes, as well as the CII-T3SS, was variable between strains, yet genes encoding the CI-T3SS were found in all isolates tested (Table 1). The presence of the CI-T3SS in all strains made it an attractive candidate as a necessary factor involved in GTPase inhibition.

To determine the involvement of the CI-T3SS in Rho family GTPase inhibition, a nonpolar deletion was generated within the *vscN1* gene encoding the homologue of the ATPase portion of the secretion apparatus in *Yersinia* spp. (38). The ability to inhibit Rho family GTPase activation was abrogated upon infection with the strain BCC23Δ*vscN1*, as activated Rho, Rac, and Cdc42 were detected during the entire course of infection (Fig. 2, left panels) and were still detectable after 8 h of infection (data not shown). Complementation with plasmid-encoded *vscN1* resulted in the partial restoration of GTPase inhibition (data not shown). A mutant strain (BCC23Δ*vscN2*) lacking the ATPase homologue of the CII-T3SS showed no deficiency in the ability to inhibit Rho family GTPase activation (Fig. 2, right panels) compared to wild-type BCC23. These findings indicate that Rho family GTPase inhibition is dependent on the secretion of bacterial effectors delivered through the CI-T3SS but not the CII-T3SS.

GTPase inhibition requires translocation of the CI-T3SS effector Vp1686. As the inhibition of Rho family GTPases is dependent on a functional CI-T3SS, we used a genetic approach to determine the secreted factor required for this effect. Three proteins, Vp1680, Vp1686, and Vpa0450, have previously been identified as CI-T3SS effectors secreted by the Asian pandemic strain RMD2210633 (50). Due to the genetic variability between North American and Asian strains of *V. parahaemolyticus*, we examined the secretion profile of BCC23. SDS-PAGE followed by matrix-assisted laser desorption ionization–time of flight mass spectrometry analysis of secreted

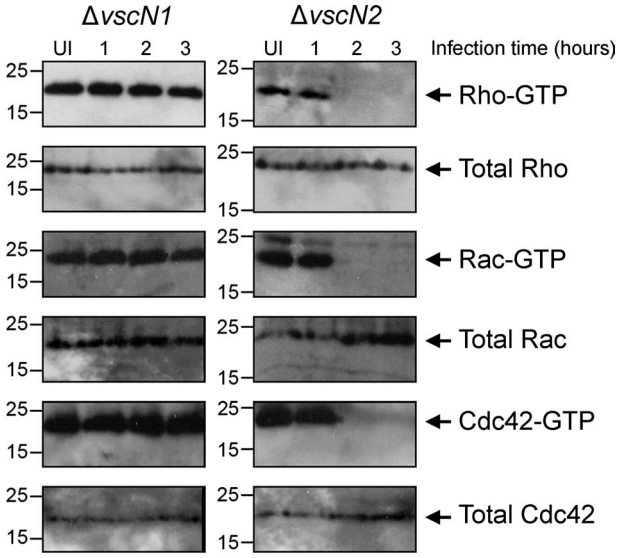

FIG. 2. The inhibition of Rho family GTPase activation is dependent on the CI-T3SS. Anti-Rho, anti-Rac, and anti-Cdc42 immunoblots of HeLa cell lysates after infection with either the CI-T3SS mutant BCC23Δ*vscN1* (Δ*vscN1*, left panels) or the CII-T3SS mutant BCC23Δ*vscN2* (Δ*vscN2*, right panels) for the indicated times. In all cases, lysates were incubated with GTPγS. Upper panels represent activated GTPase, whereas lower panels represent total cellular GTPase levels. Apparent molecular weight is in kilodaltons. Data shown are representative of three independent experiments.

proteins revealed the presence of all three proteins, including Vp1686 (data not shown).

A mutant strain lacking the secreted protein Vp1686 was unable to inhibit the activation of Rho family GTPases isolated from HeLa cells, as active Rho, Rac, and Cdc42 GTPases were detected during the entire course of infection with BCC23Δ Vp1686 (Fig. 3A, left panels). The deletion of Vp1686 did not have polar effects on the secretion of other CI-T3SS effector proteins (data not shown), indicating that the secretion of Vp1686 is necessary for GTPase inhibition. Complementation with plasmid-encoded Vp1686-HA completely restored the ability of *V. parahaemolyticus* to inhibit Rho family GTPase activation as Rho, Rac, and Cdc42 were no longer detectable after a 2-h infection (Fig. 3A, right panels). Additionally, BCC23ΔVp1686 did not inhibit the level of calpeptin-mediated Rho activation in vivo compared to that of uninfected HeLa cell monolayers, whereas complementation with Vp1686-HA restored the ability to inhibit Rho activation (Fig. 3B). A protein BLAST analysis of Vp1686 revealed that amino acid residues 348 to 355 located in the C-terminal portion of this protein encode a conserved motif, HPF*XX*GNG, called Fic (*f*ilamentation *i*nduced by *c*yclic AMP) (9). This motif is present in a family of proteins thought to be involved in the regulation of cell division, although the molecular function of these proteins has not been elucidated. It was recently reported that Vp1686 can bind directly to the nuclear protein NF-κB and that the deletion of the Fic motif does not affect this phenotype (9). To determine whether the deletion of this region had an effect on Rho inhibition, BCC23ΔVp1686 was complemented with plasmid-encoded Vp1686-HA possessing the deletion of residues 352 to 355 contained within the Fic

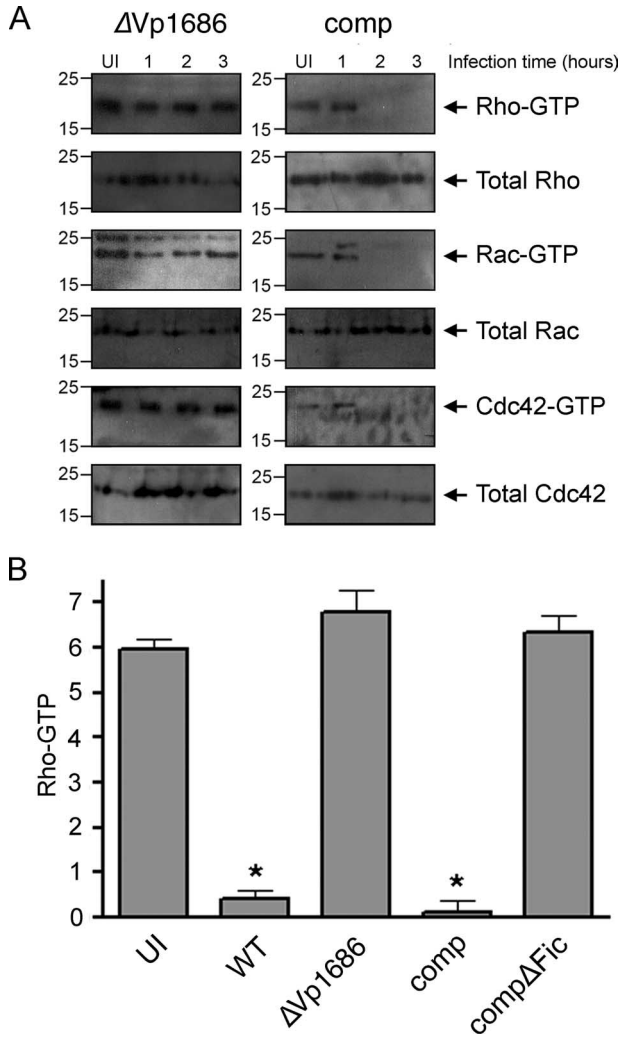

FIG. 3. The CI-T3SS effector Vp1686 is required for Rho family GTPase inhibition. (A) Anti-Rho, anti-Rac, and anti-Cdc42 immunoblots of HeLa cell lysates after infection with either BCC23ΔVp1686 (ΔVp1686, left panels) or BCCΔVp1686-comp expressing plasmid-encoded Vp1686-HA (comp, right panels) for the indicated times. In all cases, lysates were incubated with GTPγS. Upper panels represent activated GTPase, whereas lower panels represent total cellular GTPase levels. Apparent molecular weight is in kilodaltons. Data shown are representative of three independent experiments. (B) Activated Rho recovered from lysates of calpeptin-treated HeLa cells, as determined by ELISA. Cell monolayers were infected with BCC23 (wild type [WT]), BCC23ΔVp1686 (ΔVp1686), BCC23ΔVp1686-comp (comp), and BCC23ΔVp1686-compΔFic (compΔFic) for 2.5 h prior to treatment with calpeptin. Relative amounts of activated Rho are shown as a ratio of uninfected cells treated with medium control (DMSO) alone ± SEM ($n = 3$). *, $P < 0.001$ by ANOVA.

motif (BCC23ΔVp1686-compΔFic). Complementation with Vp1686ΔFic-HA did not restore the ability to inhibit Rho (Fig. 3b), indicating that an intact Fic motif is necessary for Vp1686-dependent Rho inhibition.

Vp1686 has previously been shown to be translocated into HeLa cells by the pandemic strain RMD2210633 (50). As there is considerable variability between Asian and North American isolates of *V. parahaemolyticus*, the ability of BCC23 to translocate Vp1686 was examined. Vp1686-HA was expressed in the CI-T3SS-deficient strain (BCC23Δ*vscN1*-compVp1686) as a control for the translocation of HA-tagged protein. After HeLa cell monolayers were infected, cell lysates were examined by immunoblotting. Vp1686 was detected in the membrane/cytosolic fractions of lysates from HeLa cells that had been infected with BCC23, BCC23Δ*vscN2*, BCC23ΔVp1686-comp, and BCC23ΔVp1686-compΔFic (Fig. 4A, upper panels). Vp1686 was not detected in lysates from cells infected with the gene-specific knockout strain BCC23ΔVp1686 or the CI-T3SS deletion mutant strains BCC23Δ*vscN1* and BCC23Δ*vscN1*-compVp1686 (Fig. 4A, upper panels), confirming its delivery through the CI-T3SS but not the CII-T3SS. The addition of the HA tag or the deletion of the Fic domain did not affect the translocation of Vp1686. Immunoblotting of bacterial lysates showed production of Vp1686 in all strains except the gene-specific knockout strain BCC23ΔVp1686, demonstrating that mutations affecting the secretion apparatus do not affect production of the effector protein (Fig. 4A, lower panels). Production and translocation of Vp1686 were also detected for the strains BCC34, BCC7, BCE306, and BCE515 (Fig. 4B). Taken together, our data indicate that translocation of Vp1686 is necessary for the inhibition of Rho family GTPase activation, as deficiencies in either production or translocation of this effector result in a loss of GTPase inhibition.

Rho family GTPase inhibition is coupled with an increase in the monomeric actin pool. As Rho family GTPases are important signaling molecules involved in actin dynamics, the state of cellular actin was determined in HeLa cells by using an actin sedimentation assay. Infection of HeLa cells with BCC23 resulted in an increase in the G-actin/total actin ratio compared to that of uninfected samples ($P < 0.05$; Fig. 5), indicating a shift in the total actin pool to its monomeric form. Several virulence factors of *V. parahaemolyticus* have been reported to be cytotoxic to mammalian cells (9, 31, 50, 53), which could account for a breakdown of intracellular actin structures (32). The increase in G-actin was not a result of cytotoxicity, as BCC23 did not cause an increase in lactate dehydrogenase (LDH) release after a 3-h infection compared to that of uninfected cells (uninfected [UI] = 5.35% ± 0.41% LDH release; BCC23 = 3.09% ± 0.44% LDH release; $P > 0.05$). This is consistent with our previous observation that our strain collection of *V. parahaemolyticus* causes cytoskeletal disruption in CaCo-2 cells in the absence of cytotoxicity (36). The shift observed for actin to its monomeric form is dependent on the translocation of Vp1686, as the infection with BCC23ΔVp1686 had no effect on the G-actin/total actin ratio compared to that of uninfected cells ($P > 0.05$). Complementation with Vp1686-HA restored the ability to increase the G-actin/total actin ratio ($P < 0.01$); however, complementation with Vp1686ΔFic-HA did not ($P > 0.05$, Fig. 5). Differences in total actin were not detected after infection with any of the strains ($P = 0.313$), suggesting that Vp1686 delivery causes a shift in the existing cellular actin pool to its monomeric form, rather than interfering with total actin levels. Collectively, our data show that the translocation of Vp1686 into HeLa cells leads to a redistribution of the cellular actin pool as well as inhibition of Rho family GTPases and that both of these phenotypes require an intact Fic motif.

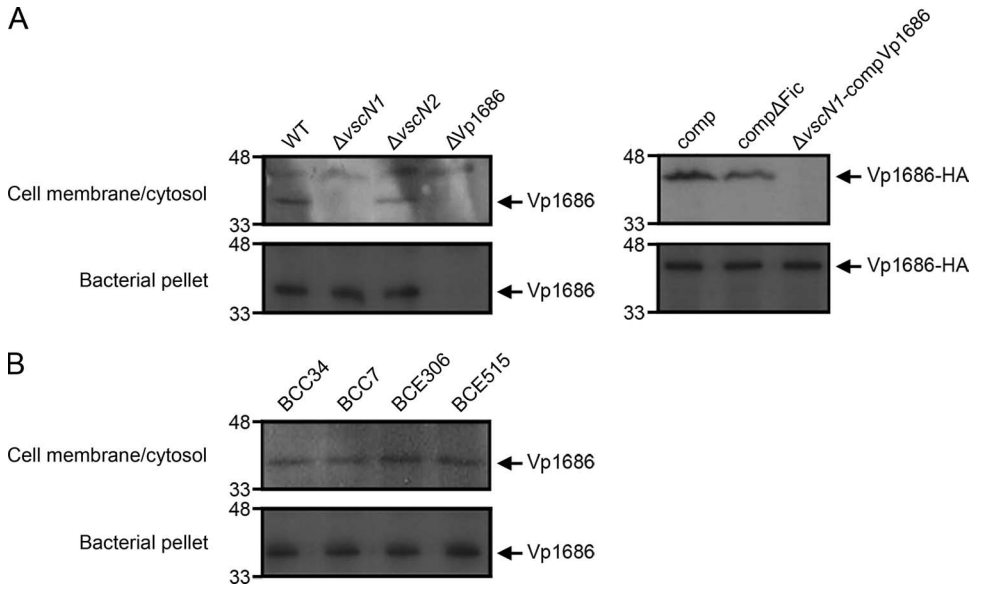

FIG. 4. Translocation of Vp1686 into HeLa cells requires the CI-T3SS. Immunoblot of infected HeLa cell lysates shows translocation of Vp1686 (upper panels) or bacterial lysates to show production of the protein (lower panels). (A) Cell lysates were probed with anti-Vp1686 after a 2.5-h infection with BCC23 (wild type [WT]), BCC23Δ*vscN1* (Δ*vscN1*), BCC23Δ*vscN2* (Δ*vscN2*), and BCC23ΔVp1686 (ΔVp1686). BCC23Δ Vp1686-comp (comp), BCC23ΔVp1686-compΔFic (compΔFic), and BCC23Δ*vscN1*-compVp1686 express HA-tagged forms of the protein, and lysates from these samples were immunoblotted with anti-HA antibody. (B) Cell lysates were probed with anti-Vp1686 after a 2.5-h infection with BCC34, BCC7, and BCE306 or an 8-h infection with BCE515. Apparent molecular weight is in kilodaltons.

DISCUSSION

This study supports previous claims that Vp1686 is a potential virulence factor of *V. parahaemolyticus*, and describes a novel effect of this translocated protein on cultured HeLa cells. We have shown that upon the cells' infection with clinical and environmental isolates of *V. parahaemolyticus*, the translocation of Vp1686 via the CI-T3SS leads to the inhibition of Rho family GTPases. This effect is independent of the CII-T3SS and the hemolytic toxins. At present, studies of potential virulence factors have been restricted largely to clinical isolates possessing the CII-T3SS and the *tdh* gene (9, 31, 34, 61). As some clinical isolates lack the genes for these effectors (39), our findings may provide insight into the virulence mechanisms used by these strains. Furthermore, the ability of environmental isolates to inhibit Rho family GTPases may indicate the potential of these strains to cause disease in susceptible hosts.

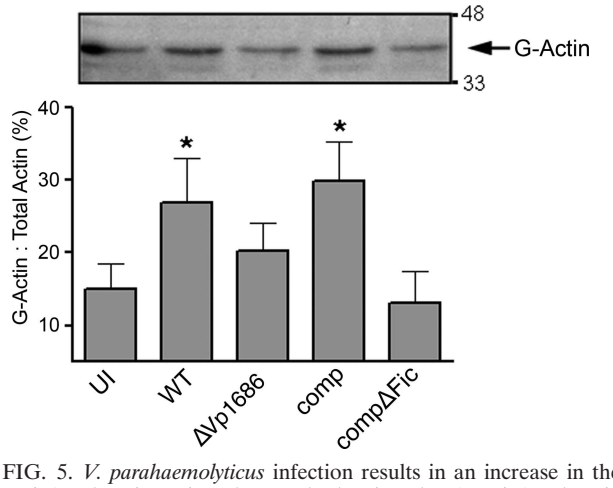

FIG. 5. *V. parahaemolyticus* infection results in an increase in the G-actin/total actin ratio. The graph showing the G-actin/total actin ratios from UI HeLa cells and HeLa cells infected with BCC23 (wild type [WT]), BCC23ΔVp1686 (ΔVp1686), BCC23ΔVp1686-comp (comp), and BCC23ΔVp1686-compΔFic (compΔFic) as measured by densitometry of anti-actin immunoblots ± SEM ($n = 4$). *, $P < 0.05$ by ANOVA. An anti-actin immunoblot of G-actin from a representative experiment is shown above. Apparent molecular weight is in kilodaltons.

The inhibition of host cell GTPases is a common mechanism of virulence among pathogenic bacteria (1, 4, 20, 30). After infection with *V. parahaemolyticus*, HeLa cells do not activate intracellular Rho in response to stimulation with calpeptin. This effect is not due to interference at the level of the stimulus itself, since in vitro activation of Rho family GTPases isolated from cell lysates is also inhibited. Total levels of cellular Rho, Rac, and Cdc42 GTPases remain unchanged during infection, indicating that the production and stability of the proteins are unaffected. Although many bacterial factors inhibit Rho family GTPases via GAP activity (21, 33), it is unlikely that this is the mechanism of Vp1686-dependent GTPase inhibition. As the pulldown assays used in this study involved the incorporation of GTPγS, a nonhydrolyzable GTP analogue, increased GAP activity would not affect the level of activated Rho family GTPases in the sample. It is possible that *V. parahaemolyticus* interferes with the incorporation of GTP either by directly targeting the GTPase itself or indirectly by targeting accessory molecules such as cellular GEFs or GDIs.

Bacterial Rho-inactivating effectors have been shown to possess multiple functional domains. ExoT and ExoS produced by *Pseudomonas aeruginosa* are bifunctional proteins capable of both inactivating Rho family GTPases via GAP activity and

interfering with other host signaling molecules via ADP ribosylation. The dual action of these proteins is separated into distinct functional domains (21, 33). Recent characterization of Vp1686 has suggested that the N-terminal region is capable of directly binding NF-κB, which may lead to apoptosis in macrophages, and that the C-terminal region containing the Fic motif is not necessary for this binding (9). Conversely, we have shown that a deletion within the Fic motif results in a loss of Rho inhibition. Deletion of these amino acids does not affect the production or translocation of stable protein into HeLa cells. Further mutational analysis is required to determine if the deletion of this region causes a loss of function directly or if the effect is indirectly due to a potential, localized improper folding of the C-terminal portion of the protein. Though it is not known whether the Fic motif is directly involved in GTPase inhibition, these observations suggest that Vp1686 may possess distinct regions required for both NF-κB binding and the inhibition of Rho family GTPases.

Bacterial pathogens hijack Rho family GTPases with various consequences to host cells, most notably involving the organization of the actin cytoskeleton (23). We have shown that the infection of cells with the clinical isolate BCC23 results in a shift in the total pool of actin to its monomeric form, which is dependent on the delivery of Vp1686 into the cell. This change in the organization of the actin cytoskeleton is independent of cytotoxicity, indicating that pathways modulating cytoskeletal dynamics are being targeted specifically. Additionally, mutation within the Fic motif interferes with GTPase inhibition and also restores the G-actin/total actin ratios to levels comparable to that of uninfected cells. Active Rho, Rac, and Cdc42 GTPases stimulate the polymerization of G-actin to F-actin during the formation of stress fibers, lamellipodia, and filopodia, respectively (28), and the inactivation of Rho family GTPases has been shown to hinder the ability of cells to form these polymerized actin structures (44, 54, 55). The ability of BCC23 to cause an overall shift in intracellular actin to its monomeric form is consistent with a decreased ability of the HeLa cells to form actin filaments as a downstream effect of Vp1686-dependent GTPase inhibition.

Although the translocation of Vp1686 contributes to the disruption of actin dynamics in HeLa cells, cytoskeletal disruption by *V. parahaemolyticus* may be multifactorial. A recent study suggests that some strains of *V. parahaemolyticus* may usurp the regulation of actin assembly by more complex mechanisms. The CI-T3 secreted protein VopL has been shown to stimulate the polymerization of actin filaments in HeLa cells by mimicking eukaryotic actin-nucleating proteins acting downstream of the Rho family GTPases (34). Type III secreted effectors exhibiting antagonistic functions are known to be utilized in concert by bacterial pathogens in order to facilitate virulence. The *Salmonella* sp. effectors SopE and SptP exhibit GEF and GAP activity, respectively, and the temporal separation of the translocation and activation of these proteins allows the sequential activation and inactivation of Rho family GTPases during the invasion process (56). It is possible that strains of *V. parahaemolyticus* possessing both CI- and CII-T3SS have developed a mechanism to promote virulence by utilizing both Vp1686 and VopL in order to control the amount of polymerized actin within the cell. The ability to inhibit Rho family GTPases is maintained in strains lacking the CII-T3SS, however, indicating that this phenotype can contribute to virulence in the absence of CII-T3SS effectors.

Cytoskeletal disruption leading to a breakdown of barrier function in epithelial cells is a well-characterized consequence of Rho family GTPase inactivation (12, 28). While Vp1686 translocation contributes to the cytoskeletal disruption observed in HeLa cells by altering the dynamics of actin polymerization, the inhibition of Rho family GTPase activation may also mediate other virulence phenotypes. Type III secreted proteins have been shown to target Rho family GTPases in order to facilitate the invasion of bacteria into host cells (49, 51), and it has been suggested that these signaling molecules may be involved in the invasion process by the *V. parahaemolyticus* clinical isolate AQ4023 (2). In contrast, our observations show that BCC23 is not invasive (unpublished data), suggesting that GTPase inhibition may be involved in yet another aspect of virulence. The inactivation of Rho family GTPases and their downstream effectors have also been shown to inhibit the phagocytic abilities of macrophages (10, 19) and to promote apoptosis in various cell lines (11, 22, 42). Fiorentini et al. have proposed a mechanism that describes how bacterial type III secreted effectors that inhibit Rho family GTPases may have both antiphagocytic and apoptotic effects in macrophages (18). This is a potential virulence mechanism of *V. parahaemolyticus*, as our preliminary data suggest that BCC23 can cause Rho inhibition in J774.1 macrophages (data not shown). Further characterization will determine the role of GTPase inhibition in various cell lines in order to better understand the contributions of this phenotype to virulence.

This study has demonstrated the ability of *V. parahaemolyticus* to disrupt host cell signaling through the inactivation of Rho family GTPases and the consequential redistribution of intracellular actin. Although the relevance of this phenotype to virulence is not yet known, future studies investigating the mechanism of GTPase inhibition and the cell types targeted will enable greater understanding of pathogenesis. There is tremendous genetic diversity among strains of *V. parahaemolyticus* (39; R. DeVinney, unpublished data), and what bacterial factors are required to cause disease in humans is currently unknown. Although much of the *V. parahaemolyticus* research has been restricted to the Asian pandemic strains, we examined a variety of North American strains for their effects on GTPases to better understand the bacterial factors involved in virulence. GTPase inhibition was observed regardless of the presence of the genes for TDH, TRH, or the CII-T3SS. As the presence of the *tdh* gene is currently used to identify pathogenic strains, we have further illustrated that a better understanding of *V. parahaemolyticus* virulence factors is essential for the proper screening of potentially pathogenic isolates.

ACKNOWLEDGMENTS

We thank Jennifer Liu and Enrico Buenaventura (Canadian Food Inspection Agency) for the strains used in this study. We also thank Emma Allen-Vercoe for the pONG expression vector.

Research in the DeVinney laboratory is supported by grants from the Natural Sciences and Engineering Research Council of Canada (NSERC) and the Canadian Institutes for Health Research (CIHR).

T.L. held an NSERC PGSD doctoral scholarship during this study. R.D. is an Alberta Heritage Foundation for Medical Research senior scholar.

REFERENCES

1. **Aepfelbacher, M., R. Zumbihl, and J. Heesemann.** 2005. Modulation of Rho GTPases and the actin cytoskeleton by YopT of *Yersinia*. Curr. Top. Microbiol. Immunol. **291:**167–175.
2. **Akeda, Y., K. Nagayama, K. Yamamoto, and T. Honda.** 1997. Invasive phenotype of *Vibrio parahaemolyticus*. J. Infect. Dis. **176:**822–824.
3. **Aktories, K.** 1997. Bacterial toxins that target Rho proteins. J. Clin. Investig. **99:**827–829.
4. **Aktories, K., and I. Just.** 2005. Clostridial Rho-inhibiting protein toxins. Curr. Top. Microbiol. Immunol. **291:**113–145.
5. **Baldwin, M. R., and J. T. Barbieri.** 2005. The type III cytotoxins of *Yersinia* and *Pseudomonas aeruginosa* that modulate the actin cytoskeleton. Curr. Top. Microbiol. Immunol. **291:**147–166.
6. **Barker, W. H., Jr., and E. J. Gangarosa.** 1974. Food poisoning due to *Vibrio parahaemolyticus*. Annu. Rev. Med. **25:**75–81.
7. **Begum, R., E. K. M. S. Nur, and M. A. Zaman.** 2004. The role of Rho GTPases in the regulation of the rearrangement of actin cytoskeleton and cell movement. Exp. Mol. Med. **36:**358–366.
8. **Bernard, O.** 2007. Lim kinases, regulators of actin dynamics. Int. J. Biochem. Cell. Biol. **39:**1071–1076.
9. **Bhattacharjee, R. N., K. S. Park, Y. Kumagai, K. Okada, M. Yamamoto, S. Uematsu, K. Matsui, H. Kumar, T. Kawai, T. Iida, T. Honda, O. Takeuchi, and S. Akira.** 2006. VP1686, a *Vibrio* type III secretion protein, induces toll-like receptor-independent apoptosis in macrophage through NF-kappaB inhibition. J. Biol. Chem. **281:**36897–36904.
10. **Black, D. S., and J. B. Bliska.** 2000. The RhoGAP activity of the *Yersinia pseudotuberculosis* cytotoxin YopE is required for antiphagocytic function and virulence. Mol. Microbiol. **37:**515–527.
11. **Bobak, D., J. Moorman, A. Guanzon, L. Gilmer, and C. Hahn.** 1997. Inactivation of the small GTPase Rho disrupts cellular attachment and induces adhesion-dependent and adhesion-independent apoptosis. Oncogene **15:**2179–2189.
12. **Bruewer, M., A. M. Hopkins, M. E. Hobert, A. Nusrat, and J. L. Madara.** 2004. RhoA, Rac1, and Cdc42 exert distinct effects on epithelial barrier via selective structural and biochemical modulation of junctional proteins and F-actin. Am. J. Physiol. Cell Physiol. **287:**C327–C335.
13. **DePaola, A., C. A. Kaysner, J. Bowers, and D. W. Cook.** 2000. Environmental investigations of *Vibrio parahaemolyticus* in oysters after outbreaks in Washington, Texas, and New York (1997 and 1998). Appl. Environ. Microbiol. **66:**4649–4654.
14. **DePaola, A., J. Ulaszek, C. A. Kaysner, B. J. Tenge, J. L. Nordstrom, J. Wells, N. Puhr, and S. M. Gendel.** 2003. Molecular, serological, and virulence characteristics of *Vibrio parahaemolyticus* isolated from environmental, food, and clinical sources in North America and Asia. Appl. Environ. Microbiol. **69:**3999–4005.
15. **Eden, S., R. Rohatgi, A. V. Podtelejnikov, M. Mann, and M. W. Kirschner.** 2002. Mechanism of regulation of WAVE1-induced actin nucleation by Rac1 and Nck. Nature **418:**790–793.
16. **Edwards, D. C., L. C. Sanders, G. M. Bokoch, and G. N. Gill.** 1999. Activation of LIM-kinase by Pak1 couples Rac/Cdc42 GTPase signalling to actin cytoskeletal dynamics. Nat. Cell Biol. **1:**253–259.
17. **Fehr, D., S. E. Burr, M. Gibert, J. d'Alayer, J. Frey, and M. R. Popoff.** 2007. Aeromonas exoenzyme T of Aeromonas salmonicida is a bifunctional protein that targets the host cytoskeleton. J. Biol. Chem. **282:**28843–28852.
18. **Fiorentini, C., L. Falzano, S. Travaglione, and A. Fabbri.** 2003. Hijacking Rho GTPases by protein toxins and apoptosis: molecular strategies of pathogenic bacteria. Cell Death Differ. **10:**147–152.
19. **Frithz-Lindsten, E., Y. Du, R. Rosqvist, and A. Forsberg.** 1997. Intracellular targeting of exoenzyme S of *Pseudomonas aeruginosa* via type III-dependent translocation induces phagocytosis resistance, cytotoxicity and disruption of actin microfilaments. Mol. Microbiol. **25:**1125–1139.
20. **Fu, Y., and J. E. Galan.** 1999. A *Salmonella* protein antagonizes Rac-1 and Cdc42 to mediate host-cell recovery after bacterial invasion. Nature **401:**293–297.
21. **Goehring, U. M., G. Schmidt, K. J. Pederson, K. Aktories, and J. T. Barbieri.** 1999. The N-terminal domain of *Pseudomonas aeruginosa* exoenzyme S is a GTPase-activating protein for Rho GTPases. J. Biol. Chem. **274:**36369–36372.
22. **Gomez, J., C. Martinez, M. Giry, A. Garcia, and A. Rebollo.** 1997. Rho prevents apoptosis through Bcl-2 expression: implications for interleukin-2 receptor signal transduction. Eur. J. Immunol. **27:**2793–2799.
23. **Gruenheid, S., and B. B. Finlay.** 2003. Microbial pathogenesis and cytoskeletal function. Nature **422:**775–781.
24. **Harlow, E., and D. Lane.** 1988. Antibodies, a laboratory manual. Cold Spring Harbor Laboratory Press, Cold Spring Harbor, NY.
25. **Ho, H. Y., R. Rohatgi, A. M. Lebensohn, M. Le, J. Li, S. P. Gygi, and M. W. Kirschner.** 2004. Toca-1 mediates Cdc42-dependent actin nucleation by activating the N-WASP-WIP complex. Cell **118:**203–216.
26. **Ho, S. N., H. D. Hunt, R. M. Horton, J. K. Pullen, and L. R. Pease.** 1989. Site-directed mutagenesis by overlap extension using the polymerase chain reaction. Gene **77:**51–59.
27. **Honda, T., Y. Ni, T. Miwatani, T. Adachi, and J. Kim.** 1992. The thermostable direct hemolysin of *Vibrio parahaemolyticus* is a pore-forming toxin. Can. J. Microbiol. **38:**1175–1180.
28. **Jaffe, A. B., and A. Hall.** 2005. Rho GTPases: biochemistry and biology. Annu. Rev. Cell Dev. Biol. **21:**247–269.
29. **Janda, J. M., C. Powers, R. G. Bryant, and S. L. Abbott.** 1988. Current perspectives on the epidemiology and pathogenesis of clinically significant *Vibrio* spp. Clin. Microbiol. Rev. **1:**245–267.
30. **Just, I., F. Hofmann, H. Genth, and R. Gerhard.** 2001. Bacterial protein toxins inhibiting low-molecular-mass GTP-binding proteins. Int. J. Med. Microbiol. **291:**243–250.
31. **Kodama, T., M. Rokuda, K. S. Park, V. V. Cantarelli, S. Matsuda, T. Iida, and T. Honda.** 2007. Identification and characterization of VopT, a novel ADP-ribosyltransferase effector protein secreted via the Vibrio parahaemolyticus type III secretion system 2. Cell. Microbiol. **9:**2598–2609.
32. **Kothakota, S., T. Azuma, C. Reinhard, A. Klippel, J. Tang, K. Chu, T. J. McGarry, M. W. Kirschner, K. Koths, D. J. Kwiatkowski, and L. T. Williams.** 1997. Caspase-3-generated fragment of gelsolin: effector of morphological change in apoptosis. Science **278:**294–298.
33. **Krall, R., G. Schmidt, K. Aktories, and J. T. Barbieri.** 2000. *Pseudomonas aeruginosa* ExoT is a Rho GTPase-activating protein. Infect. Immun. **68:**6066–6068.
34. **Liverman, A. D., H. C. Cheng, J. E. Trosky, D. W. Leung, M. L. Yarbrough, D. L. Burdette, M. K. Rosen, and K. Orth.** 2007. Arp2/3-independent assembly of actin by Vibrio type III effector VopL. Proc. Natl. Acad. Sci. USA **104:**17117–17122.
35. **Lynch, T.** 2007. Ph.D. thesis. University of Calgary, Calgary, AB, Canada.
36. **Lynch, T., S. Livingstone, E. Buenaventura, E. Lutter, J. Fedwick, A. G. Buret, D. Graham, and R. DeVinney.** 2005. *Vibrio parahaemolyticus* disruption of epithelial cell tight junctions occurs independently of toxin production. Infect. Immun. **73:**1275–1283.
37. **Maekawa, M., T. Ishizaki, S. Boku, N. Watanabe, A. Fujita, A. Iwamatsu, T. Obinata, K. Ohashi, K. Mizuno, and S. Narumiya.** 1999. Signaling from Rho to the actin cytoskeleton through protein kinases ROCK and LIM-kinase. Science **285:**895–898.
38. **Makino, K., K. Oshima, K. Kurokawa, K. Yokoyama, T. Uda, K. Tagomori, Y. Iijima, M. Najima, M. Nakano, A. Yamashita, Y. Kubota, S. Kimura, T. Yasunaga, T. Honda, H. Shinagawa, M. Hattori, and T. Iida.** 2003. Genome sequence of *Vibrio parahaemolyticus*: a pathogenic mechanism distinct from that of V cholerae. Lancet **361:**743–749.
39. **Meador, C. E., M. M. Parsons, C. A. Bopp, P. Gerner-Smidt, J. A. Painter, and G. J. Vora.** 2007. Virulence gene- and pandemic group-specific marker profiling of clinical *Vibrio parahaemolyticus* isolates. J. Clin. Microbiol. **45:**1133–1139.
40. **Michiels, T., P. Wattiau, R. Brasseur, J. M. Ruysschaert, and G. Cornelis.** 1990. Secretion of Yop proteins by *Yersiniae*. Infect. Immun. **58:**2840–2849.
41. **Miliotis, M.** 2005. Quantitative risk assessment on the public health impact of pathogenic *Vibrio Parahaemolyticus* in raw oysters. U.S. Food and Drug Administration, Washington, DC.
42. **Moorman, J. P., D. A. Bobak, and C. S. Hahn.** 1996. Inactivation of the small GTP binding protein Rho induces multinucleate cell formation and apoptosis in murine T lymphoma EL4. J. Immunol. **156:**4146–4153.
43. **Nishibuchi, M., and J. B. Kaper.** 1985. Nucleotide sequence of the thermostable direct hemolysin gene of *Vibrio parahaemolyticus*. J. Bacteriol. **162:**558–564.
44. **Nobes, C. D., and A. Hall.** 1995. Rho, rac, and cdc42 GTPases regulate the assembly of multimolecular focal complexes associated with actin stress fibers, lamellipodia, and filopodia. Cell **81:**53–62.
45. **Nolan, C. M., J. Ballard, C. A. Kaysner, J. L. Lilja, L. P. Williams, Jr., and F. C. Tenover.** 1984. *Vibrio parahaemolyticus* gastroenteritis. An outbreak associated with raw oysters in the Pacific northwest. Diagn. Microbiol. Infect. Dis. **2:**119–128.
46. **Norman, J. C., L. S. Price, A. J. Ridley, A. Hall, and A. Koffer.** 1994. Actin filament organization in activated mast cells is regulated by heterotrimeric and small GTP-binding proteins. J. Cell Biol. **126:**1005–1015.
47. **Nusrat, A., C. von Eichel-Streiber, J. R. Turner, P. Verkade, J. L. Madara, and C. A. Parkos.** 2001. *Clostridium difficile* toxins disrupt epithelial barrier function by altering membrane microdomain localization of tight junction proteins. Infect. Immun. **69:**1329–1336.
48. **Ohashi, K., K. Nagata, M. Maekawa, T. Ishizaki, S. Narumiya, and K. Mizuno.** 2000. Rho-associated kinase ROCK activates LIM-kinase 1 by phosphorylation at threonine 508 within the activation loop. J. Biol. Chem. **275:**3577–3582.
49. **Ohya, K., Y. Handa, M. Ogawa, M. Suzuki, and C. Sasakawa.** 2005. IpgB1 is a novel *Shigella* effector protein involved in bacterial invasion of host cells. Its activity to promote membrane ruffling via Rac1 and Cdc42 activation. J. Biol. Chem. **280:**24022–24034.
50. **Ono, T., K. S. Park, M. Ueta, T. Iida, and T. Honda.** 2006. Identification of proteins secreted via *Vibrio parahaemolyticus* type III secretion system 1. Infect. Immun. **74:**1032–1042.
51. **Patel, J. C., and J. E. Galan.** 2005. Manipulation of the host actin cytoskeleton by *Salmonella*: all in the name of entry. Curr. Opin. Microbiol. **8:**10–15.

52. **Pring, M., M. Evangelista, C. Boone, C. Yang, and S. H. Zigmond.** 2003. Mechanism of formin-induced nucleation of actin filaments. Biochemistry **42:**486–496.
53. **Raimondi, F., J. P. Kao, C. Fiorentini, A. Fabbri, G. Donelli, N. Gasparini, A. Rubino, and A. Fasano.** 2000. Enterotoxicity and cytotoxicity of *Vibrio parahaemolyticus* thermostable direct hemolysin in in vitro systems. Infect. Immun. **68:**3180–3185.
54. **Ridley, A. J., and A. Hall.** 1992. The small GTP-binding protein rho regulates the assembly of focal adhesions and actin stress fibers in response to growth factors. Cell **70:**389–399.
55. **Ridley, A. J., H. F. Paterson, C. L. Johnston, D. Diekmann, and A. Hall.** 1992. The small GTP-binding protein rac regulates growth factor-induced membrane ruffling. Cell **70:**401–410.
56. **Schlumberger, M. C., and W. D. Hardt.** 2005. Triggered phagocytosis by *Salmonella*: bacterial molecular mimicry of RhoGTPase activation/deactivation. Curr. Top. Microbiol. Immunol. **291:**29–42.
57. **Schoenwaelder, S. M., and K. Burridge.** 1999. Evidence for a calpeptin-sensitive protein-tyrosine phosphatase upstream of the small GTPase Rho. A novel role for the calpain inhibitor calpeptin in the inhibition of protein-tyrosine phosphatases. J. Biol. Chem. **274:**14359–14367.
58. **Sheahan, K. L., and K. J. Satchell.** 2007. Inactivation of small Rho GTPases by the multifunctional RTX toxin from Vibrio cholerae. Cell. Microbiol. **9:**1324–1335.
59. **Shirai, H., H. Ito, T. Hirayama, Y. Nakamoto, N. Nakabayashi, K. Kumagai, Y. Takeda, and M. Nishibuchi.** 1990. Molecular epidemiologic evidence for association of thermostable direct hemolysin (TDH) and TDH-related hemolysin of *Vibrio parahaemolyticus* with gastroenteritis. Infect. Immun. **58:**3568–3573.
60. **Simon, R., U. Priefer, and A. Puhler.** 1983. A broad host range mobilization system for *in vivo* genetic engineering: transposon mutagenesis in gram negative bacteria. Nat. Biotechnol. **1:**784–791.
61. **Trosky, J. E., Y. Li, S. Mukherjee, G. Keitany, H. Ball, and K. Orth.** 2007. VopA inhibits ATP binding by acetylating the catalytic loop of MKKs. J. Biol. Chem. **282:**34299–34305.
62. **Voth, D. E., and J. D. Ballard.** 2005. *Clostridium difficile* toxins: mechanism of action and role in disease. Clin. Microbiol. Rev. **18:**247–263.
63. **White, A. P., E. Allen-Vercoe, B. W. Jones, R. DeVinney, W. W. Kay, and M. G. Surette.** 2007. An efficient system for markerless gene replacement applicable in a wide variety of enterobacterial species. Can. J. Microbiol. **53:**56–62.
64. **Zigmond, S. H.** 2004. Formin-induced nucleation of actin filaments. Curr. Opin. Cell Biol. **16:**99–105.

Editor: J. B. Bliska